Purdue University
Purdue e-Pubs

International Compressor Engineering Conference

School of Mechanical Engineering

1996

Turbulent Flow Through Valves of Reciprocating Compressors

C. J. Deschamps
Federal University of Santa Catarina

R. T. S. Ferreira
Federal University of Santa Catarina

A. T. Prata
Federal University of Santa Catarina

Follow this and additional works at: https://docs.lib.purdue.edu/icec

TURBULENT FLOW THROUGH VALVES OF RECIPROCATING COMPRESSORS

C.J. Deschamps, R.T.S. Ferreira and A.T. Prata

Department of Mechanical Engineering
Federal University of Santa Catarina
88 040-900, Florianópolis/SC, BRAZIL

ABSTRACT

The present work considers the modeling of turbulent flow in reed type valves of reciprocating compressors and is based on a simplified geometry of the actual valve, that is, a radial diffuser with axial feeding. Despite its simplicity the geometry chosen for the analysis has important flow features present in practical geometries. Due to its claimed capability to predict flow including features such as recirculating region, curvature and adverse pressure gradient (all of them present in the flow considered here), the RNG k-ε model of Orzag et al. (1993) has been applied in the present numerical analysis, which is based on the finite volume methodology. Numerical results of pressure distribution along the front disc, for different valve lifts s and Reynolds numbers Re, when compared to experimental data showed that the RNG k-ε model can predict quite successfully the flow.

INTRODUCTION

Most of reciprocating compressors employ automatic valves that open and close depending on the pressure difference across them. That is particularly true for small reciprocating compressors largely used in domestic refrigerators. Usually, these are reed type valves whose design requires a deep understanding of the fluid flow through them. From the geometrical point of view a basic configuration for reed-type valves of reciprocating compressors is a radial diffuser with axial feeding. Fig. 1 presents a view of such a diffuser and details the geometric parameters that govern the flow, including a backward facing radial step. This step reduces the contact area between the valve reed and the valve seat and minimizes sticking. The basic configuration of Fig. 1 applies to both suction and discharge valves. In both cases the fluid enters the valve flowing axially through the valve port, hits the facing disk and, after being deflected by it, a radial flow is established. The impact of the flow on the facing disk produces a bell-shape pressure distribution yielding a resultant force that tends to open the valve. Depending on the gap between the disks and on the flow Reynolds number, negative pressure regions can occur which have a strong impact on both the pressure drop and the resultant force on the reed.

Despite the numerous works related to laminar radial flows, very little attention has been given to turbulent flows. For references on laminar flow the interested reader is referred to Hayashi et al. (1975), Wark and Foss (1984), Ferreira et al. (1989), Gasche et al. (1992), Prata et al. (1995) and the literature cited therein. The few works dealing with radial turbulent flow focused on pure radial flow between parallel disks without considering the inlet which is of crucial importance for valve applications (Ervin et al., 1989 and Tabatabai and Pollard, 1987).
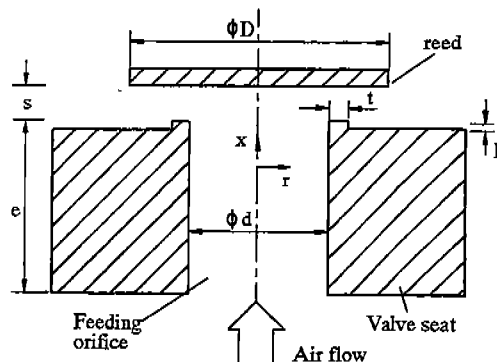
Fig. 1 - Geometry of radial diffuser with axial feeding

Apparently, the first attempt to solve the turbulent flow in axial feeding radial diffusers was made by Deschamps et al. (1988). There it was found that the High Reynolds Number k-ε model used to close the averaged Navier-Stokes equations was unable to predict the flow, even with the inclusion of correction terms to take into account effects such as flow curvature. The bad performance of the numerical solution was attributed to the wall-functions needed in the model. This was confirmed later when a Low Reynolds Number k-ε model, which does not use wall-functions, produced better flow predictions (Deschamps et al. 1989). Nevertheless, even for this model there were significant differences between experiments and computations. In reality, the k-ε turbulent model is known to produce excessive turbulence in the presence of adverse pressure gradient, as is the case at the entrance of the radial diffuser. This leads to an overprediction of turbulence intensity and to delay, or even suppress, eventual flow separations hinted at by the laboratory measurements.

The main goal of the present paper is to perform a numerical simulation with experimental validation of the turbulent flow through the geometry depicted in Fig. 1. Due to the claimed capability to predict flows that include features such as stagnation and recirculation regions, curvature and adverse pressure gradients (all of them present in the flow considered here) the k-ε model of Orzag et al. (1993) was adopted in this work.

TURBULENCE MODELING

The time/ensemble averaged Navier-Stokes equations are closed using the concept of a 'turbulent' or 'eddy' viscosity v_t. For an isothermal and incompressible flow under the effect of no body force the equations of motion (here written in Cartesian tensor notation) are:

Mass conservation,
$$\frac{\partial U_i}{\partial x_i} = 0 \quad , \tag{1}$$

Momentum conservation for the x_i component of velocity,

$$U_j \frac{\partial U_i}{\partial x_j} = -\frac{1}{\rho} \frac{\partial}{\partial x_i} \left(P + \frac{2}{3}\rho k \right) + \frac{\partial}{\partial x_j} \left[v_{eff} \left(\frac{\partial U_i}{\partial x_j} + \frac{\partial U_j}{\partial x_i} \right) \right] \tag{2}$$

where $v_{eff} (= v + v_t)$ is the effective viscosity, v $(= \mu/\rho)$ is the air kinematic viscosity and μ and ρ are the air absolute viscosity and density, respectively.

By far the most common choice for modeling v_t has been that in terms of the turbulence kinetic energy k and its rate of dissipation ε. Recently, Orzag et al. (1993) derived a model of this kind from the original governing equations for fluid using mathematical techniques called Renormalization Group (RNG) methods. Due to this mathematical foundation, Orzag and his colleagues argue that the RNG k-ε model offers a wide range of applicability. Some examples of flows where the RNG k-ε model has been seen to return better predictions than previous k-ε models are those including flow separation, streamline curvature and flow stagnation. These flow features play a crucial role in the valve efficiency and, therefore, it seemed natural to adopt the RNG k-ε model in the present work.

The effective viscosity is given by

$$v_{eff} = v \left[1 + \sqrt{\frac{C_\mu}{v}} \frac{k}{\sqrt{\varepsilon}} \right]^2 \quad , \tag{3}$$

which is valid across the full range of flow conditions from low to high Reynolds numbers. The turbulence kinetic energy k and its dissipation ε appearing in (3) are obtained from the following transport equations:

$$U_j \frac{\partial k}{\partial x_j} = \frac{\partial}{\partial x_j} \left[\alpha v_t \frac{\partial k}{\partial x_j} \right] + v_t S^2 - \varepsilon \quad , \qquad U_j \frac{\partial \varepsilon}{\partial x_j} = \frac{\partial}{\partial x_j} \left[\alpha v_t \frac{\partial \varepsilon}{\partial x_j} \right] + C_{\varepsilon 1} \frac{\varepsilon}{k} v_t S^2 - C_{\varepsilon 2} \frac{\varepsilon^2}{k} - R \quad , \tag{4}$$

The values of C_μ, $C_{\varepsilon 1}$ e $C_{\varepsilon 2}$ are equal to 0.0845, 1.42 and 1.68; respectively. The inverse Prandtl number α for turbulent transport and the rate of strain term, R, are given by the following relationships:

$$\left|\frac{\alpha - 1.3929}{\alpha_o - 1.3929}\right|^{0.6321} \left|\frac{\alpha + 2.3929}{\alpha_o + 2.3929}\right|^{0.3679} = \frac{\nu}{\nu_{eff}} \quad , \qquad R = \frac{C_\mu \eta^3 (1 - \eta / \eta_0)}{1 + \beta \eta^3} \frac{\varepsilon^2}{k} \quad , \tag{5}$$

where $\alpha_o = 1.0$, $\beta = 0.012$, $\eta = S k / \varepsilon$, $\eta_o \approx 4.38$ and $S^2 = 2 S_{ij} S_{ij}$ is the modulus of the rate-of-strain tensor. In regions of small strain rate, the term R has a trend to increase ν_{eff} somewhat, but even in this case ν_{eff} still is typically smaller than its value returned by the standard k-ε model. In regions of elevated strain rate the sign of R becomes negative and ν_{eff} is considerably reduced. This feature of the RNG k-ε is responsible for substantial improvements verified in the prediction of large separation flow regions. Also the reduced value of $C_{\varepsilon 2}$ in the RNG theory , compared to the value of 1.9 used in the standard k-ε turbulence model, acts to decrease the rate of dissipation of ε, leading to smaller values of ν_{eff} .

Boundary conditions at inlet, walls, axis of symmetry and outlet are required to solve equations (1), (2) and (4). For the inlet boundary it was recognized by Ferreira et al. (1989) that, as the flow exits the feeding orifice of area A_f and enters the diffuser of area A_d , the strong reduction of the passage area given by the ratio $A_d / A_f = 4$ s/d brings about a strong flow acceleration next to the orifice wall for small values of s/d. Due to this phenomenon the inflow velocity profile plays no role in the solution of the flow field in the diffuser and hence the inlet boundary condition was specified as $U = \overline{U}_{in}$ and V=0, where $\overline{U}_{in}$ is the average velocity in the feeding orifice. Despite no information is available for the turbulence kinetic energy, numerical tests indicated that when the level of the turbulence intensity I ($= \sqrt{\overline{uu}} / \overline{U}_{in}$) was increased from 3% to 6% no significant change was observed in the predicted flow. Therefore, a value of 3% of turbulence intensity was used in the calculation of all results shown in this work. Finally, the distribution of the dissipation rate was estimated based on the assumption of equilibrium boundary layer, that is, $\varepsilon = \lambda^{3/4} k^{3/2} / \ell_m$, where $\ell_m = 0.07$ d /2 and $\lambda = 0.09$. At the solid boundaries the condition of non-slip and impermeable wall boundary condition were imposed for the velocity components, that is, U=V=0, with calculations being extended up to the walls across the viscous sublayer. For the turbulence quantities k and ε rather than prescribing a condition at the walls, they were calculated in the control volume adjacent to the wall following a non-equilibrium wall-function. In the plane of symmetry, the normal velocity and the normal gradients of all other quantities were set to zero. At the outlet boundary, the solution domain had to be extended well beyond the diffuser exit where prevails the atmospheric pressure. The boundary condition for k in this case was fixed according to a turbulence intensity of 3% whereas the dissipation rate was estimated based on the same assumption of equilibrium boundary layer used at the inlet, as indicated above. Given the wall jet characteristic of the flow exiting the diffuser, it is expected that any eventual inaccuracy of the above outlet conditions will not have a significant impact on the numerical solution.

NUMERICAL METHODOLOGY

The numerical solution of the governing equations was performed using the commercial computational fluid dynamics code FLUENT, version 4.2 (1993). In this code the conservation equations for mass, momentum and turbulence quantities are solved using the finite volume discretization method. For this practice the solution domain is divided in small control volumes, using a non-staggered grid scheme, and the governing differential equations are integrated over each control volume with use of Gauss theorem. The resulting system of algebraic equations is solved using the Gauss-Seidel method and the SIMPLE algorithm. In the finite volume method, schemes used to evaluate property transport by convection across each volume surface can be of primary importance to the accuracy of the numerical results. In the present work, the QUICK scheme was adopted in the solution of momentum equations, yielding a second order accuracy for the interpolated values. Yet, for the transport equations of turbulence quantities the Power Law Differencing Scheme (PLDS) was adopted since the unboundness of the QUICK scheme usually introduces serious numerical instabilities, causing calculations to diverge. Different grid levels were tested in the computation to guarantee a grid independent numerical solution. The refinement was mainly promoted in the entrance of the diffuser, where flow property gradients are steeper. Of great help to this test was some evidence of the discretization needed for the analysis and made available by Deschamps et al. (1989). The final computational grid used for the numerical predictions consisted of 70 and 80 nodes in the axial and radial directions, respectively.

RESULTS AND DISCUSSIONS

The flow through the valve reed in Fig. 1 is investigated for three valve lifts s/d (=0.05, 0.07 and 0.10) and two Reynolds numbers, $Re = \rho \bar{U}_{in} d / \mu$, (=10,000 and 40,000). Additionally, the effect of a backward facing radial step in the valve seat was also considered (p/d=0.039 and t/d=0.138, according to Fig. 1). A careful experimental setup was built to measure the pressure distribution on the valve seat as a function of the Reynolds number and the valve lift. Of paramount importance in the experiments was the correct adjustment of the valve lift to the desired value due to the strong influence of this parameter on the flow field. A detailed description of both the experimental setup and procedure will not be presented here due to space limitations but can be found in Ferreira et al. (1989).

Fig. 2 shows the radial distribution of dimensionless pressure P^* ($= 2P / \rho \bar{U}_{in}^2$) on the valve surface obtained from the experiments and computations, for a flow geometry without and with the backward step in the valve seat (Fig.2a and Fig.2b, respectively). In both situations there is a plateau of pressure on the central part of the curve (r/d < 0.5), as previously verified for the laminar flow by Ferreira et al. (1989). Also similar to the laminar flow is the sharp pressure drop at the radial position r/d ≈ 0.5, which is due to the change of the flow direction. For the outer part of the curve (r/d>0.5) the pressure level never recovers a positive value, a situation which is also verified in the laminar flow for combinations of large valve lift and Reynolds number. In fact, for the situations shown, the pressure even at the exit of the diffuser is seen not to reach the atmospheric condition, remaining negative. The presence of negative levels of pressure may prevent the perfect valve operating conditions since it reduces the resultant force acting on the reed surface. The effect on the flow of the backward facing radial step is small. However, a careful examination of Fig. 2 suggests, as a consequence of the step, a small increase in the pressure values for r/d>0.5 that yields an increase of the force on the valve reed. The good agreement between experiments and computations typically pictured in Fig. 2, which were similar to several other situations of valve lift and Reynolds number, provided confidence on the turbulence model. Thus, the next step in the analysis was to generate numerical simulations for flow situations not included in the experimental investigation. The computations were then conducted for three valve lifts s/d (=0.05; 0.07 and 0.10) and two Reynolds numbers Re (= 10,000 and 40,000) for the valve reed geometry without the backward facing radial step. The results plotted in Fig. 3 at first sight show no significant difference between the pressure distributions on the valve surface for the two Reynolds numbers explored. However, a first distinction between the curves is that for increasing Re values, the magnitude of the negative pressure profiles decreases. Another important detail of the flow is disclosed with the help of Fig. 4. There, the pressure distributions of Re = 10,000 and 40,000, normalized by the pressure value P_0 at the center of the valve (r/d=0), are presented for two valve lifts: s/d =0.05 and 0.10. The figure shows that the pressure drop at r/d ≈ 0.5 is more pronounced for smaller valve lifts. This is an expected result since as the valve lift increases the change in the flow direction at r/d ≈ 0.5 is less stiff. Additionally, for s/d=0.05 an increase in the Reynolds number brings about a considerable enhancement of the negative region in the pressure distribution, whereas, for s/d=0.10, the Reynolds number effect in the shape of the pressure distribution is much less prominent.
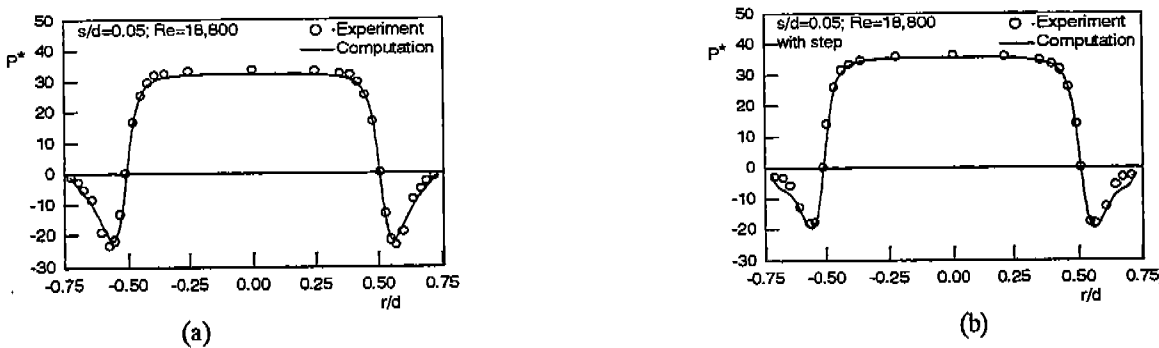

(a)   (b)

Fig. 2 - Typical numerical and experimental results for pressure distribution on the valve reed

The force F acting on the valve surface is obtained by integrating the pressure distribution on the reed surface. Fig. 5a represent the dimensionless force F^* ($= 2F / \rho \bar{U}_{in}^2 A_f$) as a function of valve lift s/d for two Reynolds numbers: Re=10,000

and 40,000. For Re=10,000 there is a pronounced decay in the force when s/d is varied from 0.05 to 0.07. This is mainly associated with the strong drop in the pressure level on the central region of the valve (r/d<0.5) that occurs as the valve lift is increased. In the case of Re=40,000, the decay is less pronounced because of the fading of the pressure negative region that occurs as the lift is increased, which offsets the reduction in the stagnation pressure.

The force needed to compute the valve movement in compressor simulation programs is usually obtained via the effective force area, A_{ef}. From the pressure difference across the valve, $\Delta p = p_u - p_d$ (upstream - downstream pressure), A_{ef} is determined from $A_{ef} = F/\Delta p$. Plots of dimensionless A^*_{ef} ($= A_{ef}/A_f$) as a function of s/d are shown in Fig. 5b for two Reynolds numbers. As can be seen from the figure, the most interesting change in A^*_{ef} is observed for Re=40,000 when the valve lift is changed from s/d=0.05 to 0.07. This rise in A^*_{ef} is an outcome from the substantial decline in the negative pressure levels as the valve lift is increased.

The effective flow area, A_{ee}, is an useful parameter in the valve design and is related to the pressure drop through the valve. Given a pressure drop, A_{ee} can yield the mass flow rate $\dot{m}$ across the valve. The higher A_{ee} the lesser the loss of flow energy and, therefore, the better the valve performance. The effective flow area is defined as:

$$A_{ee} = \dot{m} \left/ \left\{ p_u \left[\frac{2k}{(k-1)RT_u} \right]^{1/2} \left[r^{2/k} - r^{(k+1)/k} \right]^{1/2} \right\} \right. \quad .$$

(6)

In the equation above $r = p_{atm}/p_u$, $k = c_p/c_v$ and $R = c_p - c_v$. On the other hand, p_u and T_u are the pressure and temperature upstream the feeding orifice, p_{atm} is the atmospheric pressure and c_p and c_v are the air specific heats. Plots of dimensionless A^*_{ee} ($= A_{ee}/A_f$) are shown in Fig. 5c. In that figure one can see that as the valve lift is increased the efficiency of the valve in conducting the fluid also increases. On the other hand, as the Reynolds number becomes greater, the efficiency becomes smaller; probably due to the presence of larger recirculating regions in the valve passage.
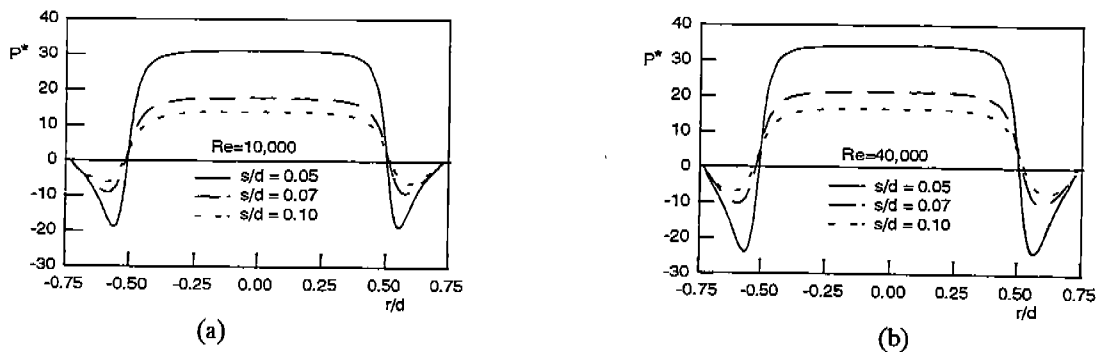

Fig. 3 - Numerical results for pressure distribution on the valve reed; no step on the seat.
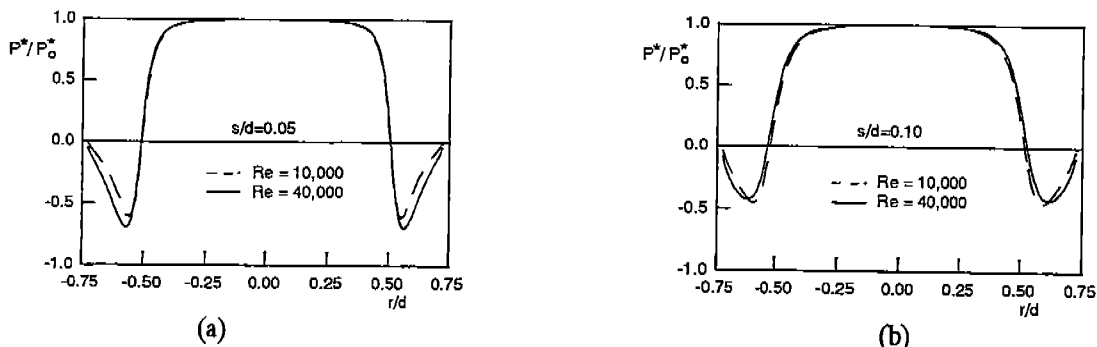

Fig. 4 - Results of normalized pressure distributions on the valve reed; no step on the seat.
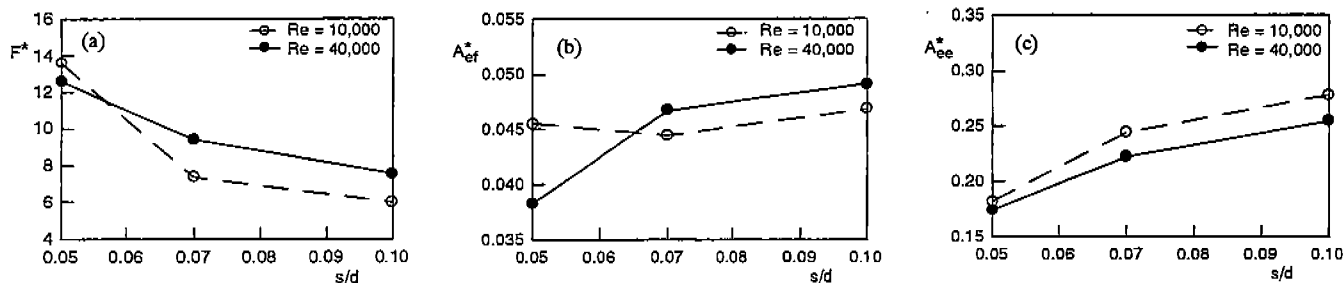
Fig. 5 - Dimensionless force, effective force area and effective flow area; no step on the seat.

CONCLUSIONS

The present work has presented a numerical and experimental investigation of the incompressible turbulent and isothermal flow in radial diffuser. This is the basic flow problem associated to automatic valve reeds of reciprocating compressors. The flow was analyzed for different parameters such as Reynolds number and gap between the disks. The RNG k-ε turbulence model used to predict the flow was found to reproduce well the experimental results. One of the main features observed in all flow situations is the presence of pressure negative levels along the entire diffuser on the valve surface. For the cases investigated here, it seems that as the gap between the disks is increased the shape of the pressure distribution on the valve surface becomes less and less dependent on the Reynolds number and the gap itself.

ACKNOWLEDGMENTS

REFERENCES

- Deschamps, C.J., Ferreira, R.T.S. and Prata, A.T., 1988, "Application of the k-ε Model to Turbulent Flow in Compressor Valves", *Proc. 2nd Brazilian Thermal Science Meeting*, São Paulo, pp. 259-262, (in Portuguese).
- Deschamps, C.J., Prata, A.T. and Ferreira, R.T.S., 1989, "Turbulent Flow Modeling in Presence of Stagnation, Recirculation, Acceleration and Adverse Pressure Gradient", *Proc. X Brazilian Congress of Mechanical Engineering*, v. I, pp. 57-60, (in Portuguese).
- Ervin, J. S., Suryanarayana, N. V. and Ng, H. C., 1989, "Radial Turbulent Flow of a Fluid Between Two Coaxial Disks", *ASME J. Fluids Eng.*, Vol. 111, pp. 378-383.
- Hayashi, S., Matsui, T. and Ito, T., 1975, "Study of Flow and Thrust in Nozzle-Flapper Valves", *ASME J. Fluids Eng.*, Vol. 97, pp. 39-50.
- Ferreira, R. T. S., Deschamps, C. J. and Prata, A. T., 1989, "Pressure Distribution Along Valve Reeds of Hermetic Compressors", *Experimental Thermal and Fluid Sciences*, Vol. 2, pp. 201-207.
- FLUENT, 1993, Fluent Inc., Centerra Resource Park, 10 Cavendish Court, Lebanon, NH 03766.
- Gasche, J. L., Ferreira, R. T. S. and Prata, A. T., 1992, "Pressure Distributions Along Eccentric Circular Valve Reeds of Hermetic Compressors", *Proc. of the International Compressor Engineering Conference at Purdue*, West Lafayette, USA, Vol. IV, pp. 1189-1198.
- Orzag, S.A., Yakhot, V. Flannery, W.S., Boysan, F., Choudhury, D. Marusewski,J., Patel,B., 1993, "Renormalization Group Modeling and Turbulence Simulations".In So,R.M.C., Speziale,C.G., Launder, B.E. (editors), *Near-wall turbulent flows*. Elsevier Science Publisher.
- Prata, A. T., Pilichi, C. D. M. and Ferreira, R. T. S., 1995, "Local Heat Transfer in Axially Feeding Radial Flow Between Parallel Disks", *ASME J. of Heat Transfer*, Vol. 117, pp. 47-53.
- Tabatabai, M. and Pollard, A., 1987, "Turbulence in Radial Flow Between Parallel Disks at Medium and Low Reynolds Numbers", *J. Fluid Mechanics*, Vol. 185, pp. 483-502.
- Wark, C. E. and Foss, J. F., 1984, "Forces Caused by the Radial Outflow Between Parallel Disks", *ASME J. Fluids Eng.*, Vol. 106, pp. 292 - 297.